

# Microscopic features of moving traffic jams

Boris S. Kerner<sup>1</sup>, Sergey L. Klenov<sup>2</sup>, Andreas Hiller<sup>3</sup>, and Hubert Rehborn<sup>4</sup>

<sup>1, 3, 4</sup> DaimlerChrysler AG, REI/VF, HPC: G021, 71059 Sindelfingen, Germany and

<sup>2</sup> Moscow Institute of Physics and Technology, Department of Physics, 141700 Dolgoprudny, Moscow Region, Russia

Empirical and numerical microscopic features of moving traffic jams are presented. Based on a single vehicle data analysis, it is found that within wide moving jams, i.e., between the upstream and downstream jam fronts there is a complex microscopic spatiotemporal structure. This jam structure consists of alternations of regions in which traffic flow is interrupted and flow states of low speeds associated with “moving blanks” within the jam. Empirical features of the moving blanks are found. Based on microscopic models in the context of three-phase traffic theory, physical reasons for moving blanks emergence within wide moving jams are disclosed. Structure of moving jam fronts is studied based in microscopic traffic simulations. Non-linear effects associated with moving jam propagation are numerically investigated and compared with empirical results.

PACS numbers: 89.40.+k, 47.54.+r, 64.60.Cn, 64.60.Lx

## I. INTRODUCTION

Freeway traffic is a complex dynamic spatiotemporal process. A huge number of traffic flow models have been introduced for explanations of traffic phenomena (see the book [1], the reviews [2, 3, 4, 5, 6, 7, 8], and the conference proceedings [9, 10, 11, 12]).

In empirical freeway traffic observations, it has been found that traffic can be either free or congested. In congested traffic, the “stop-and-go” phenomenon is observed, i.e., a sequence of moving jams can appear (see the classic papers by Edie and Foote, Treiterer et al., Koshi et al. [13, 14, 15, 16, 17, 18]). A moving jam is a localized structure propagating upstream. The jam is spatially restricted by two jam fronts in which the speed, density, and flow rate vary sharply. Within the upstream jam front, vehicles must decelerate to the speed in the jam. Within the downstream jam front, vehicles accelerate escaping from the jam.

Recently, from spatiotemporal analysis of empirical data measured over many days and years on various freeways in different countries, Kerner found that there are two different phases in congested traffic, synchronized flow and wide moving jam (see references in the book [1]). Thus, there are three traffic phases: 1. Free flow. 2. Synchronized flow. 3. Wide moving jam.

The fundamental difference between synchronized flow and wide moving jam is determined by the following macroscopic spatiotemporal objective (empirical) criteria, which define the phases [1]. The wide moving jam is a moving jam that exhibits the *characteristic, i.e., unique, and coherent feature* to maintain the mean velocity of the downstream jam front, even when the jam propagates through any other traffic states or freeway bottlenecks. In contrast, synchronized flow does not exhibit this characteristic feature, in particular, the downstream front of synchronized flow is often *fixed* at a freeway bottleneck.

Wide moving jam propagation through a freeway bottleneck is associated with traffic flow interruption within the jam: Vehicles are in a stop within the jam during a time interval, which is considerably longer than the mean

time delay in vehicle acceleration at the downstream jam front. Thus, flow interruption within wide moving jams can be used as a microscopic criterion for distinguishing between the wide moving jams and synchronized flow in congested traffic, even if single vehicle data is measured at a single freeway location [19]. The traffic flow interruption effect discloses the physical nature of a qualitatively different behavior of the wide moving jam phase in comparison with the synchronized flow phase. Moreover, from an analysis of wide moving jams it can be assumed that there are moving blanks within the jams: Vehicles come to a stop at different net distances (space gaps) to each other at the upstream front of a wide moving jam. Later, vehicles begin to move within the jam to cover these blanks within the jam; as a result blanks appear that move against the flow.

It can be expected that both flow interruption within the jams and moving blanks should influence microscopic features and characteristics of moving jams considerably. However, a microscopic spatiotemporal structure of moving jams, in particular, the effect of moving blanks as well as microscopic features of the jam fronts have not been understood. In this paper, based on an empirical single vehicle data analysis the microscopic spatiotemporal structure of moving jams and its microscopic features have been found. These empirical features have been explained using numerical simulations of a microscopic model in the context of three-phase traffic theory, which is adequate with all known empirical observations of congested traffic [1]. The article is organized as follows. Empirical and theoretical features of moving blanks within wide moving jams are considered in Sect. II. In Sect. III, microscopic features of the jam fronts and jam propagation are numerically studied.

## II. MOVING BLANKS WITHIN WIDE MOVING JAMS

### A. Microscopic Characteristics of Moving Blanks in Empirical Single Vehicle Data

#### 1. Congested States in Single Vehicle Data

Single vehicle characteristics are usually obtained either in driver experiments or through the use of detectors (e.g., [18, 20, 21, 22, 23, 24, 25, 26, 27, 28]). In the latter case, data from a single freeway location or aggregated data measured at different locations are used [29].

Single vehicle data used in the article have been measured on two different freeways in Germany. The first single vehicle data set has been measured on the three-lane freeway section of the freeway A5-South at detectors 10 and 7 (Fig. 1 (a)); a detailed consideration of this freeway section is made in [30]. For an overview of moving jams observed in single vehicle data and used below, the data averaged over 1-min intervals are shown in Fig. 1 (b). The second set of single vehicle data has been measured on a two-lane section of the freeway A92-West at detectors D1 and D2 between intersections “AS Freising-Süd” (I2) and “AK Neufahrn” (I3) near Munich Airport (intersection I1: “AS Flughafen” in Fig. 1 (c)). Local dynamics of the average speed and flow rate (1-min averaged data) for two typical days at which congested traffic have been observed are shown in Fig. 1 (d, e).

In both freeway sections, single vehicle data are measured through the use of two sets of double induction loop detectors. A detector set consists of two detectors for each of the freeway lanes. A detector registers a vehicle by producing a current electric pulse whose duration  $\Delta t_i$  is related to the time taken by the vehicle to traverse the induction loop. This enables us to calculate the gross time gap between two vehicles  $i$  and  $i+1$  that have passed the loop one after the other  $\tau_{i,i+1}^{(\text{gross})}$ . There are two detector loops in each detector. The distance between these loops is constant. This enables us to calculate the individual vehicle speed  $v_i$  and estimate the vehicle length  $d_i = v_i \Delta t_i$  as well as the net time gap (time headway) between the vehicles  $i$  and  $i+1$ :  $\tau_{i,i+1} = \tau_{i,i+1}^{(\text{gross})} - \Delta t_i$ .

#### 2. Alternations of Flow Interruption and Moving Blanks within Moving Jams

Within wide moving jams, i.e., between the jam fronts regions in which flow is interrupted are alternated with moving blanks (Fig. 2). The condition for flow interruption is [19]:

$$\tau_{\text{max}} \gg \tau_{\text{del}}^{(\text{ac})}, \quad (1)$$

where  $\tau_{\text{max}}$  is the maximum time headway between two vehicles within the jam and  $\tau_{\text{del}}^{(\text{ac})}$  is the mean time delay in vehicle acceleration at the downstream jam front from

a standstill state within the jam. Under the condition (1), there are at least several vehicles within the jam that are in a standstill or if they are still moving, it is only with a negligible low speed in comparison with the speed in the jam inflow and outflow. These vehicles separate vehicles accelerating at the downstream jam front from vehicles decelerating at the upstream jam front: The inflow into the jam has no influence on the jam outflow. Then the jam outflow is fully determined by vehicles accelerating at the downstream jam front. In the example, flow interruption effect occurs two times during jam propagation through detector D10 [33] (Fig. 2 (a–g)); these time intervals are labeled “flow interruption” in Fig. 2 (g)). The values  $\tau_{\text{max}}$  for the first flow interruption intervals within the wide moving jam are equal to approximately 50 s in the left lane, 30 s in the middle line, and 80 s in the right line. These values  $\tau_{\text{max}}$  satisfy the criterion (1) because corresponding to empirical results  $\tau_{\text{del}}^{(\text{ac})} \approx 1.5 - 2$  sec [1].

Whereas the first flow interruption interval appears almost simultaneously in all freeway lanes, the second one occurs in the left lane earlier than in the middle and right lanes (Fig. 2 (a–g)). In other empirical examples of wide moving jams, the flow interruption effect occurs in some of the freeway lanes only whereas in other lane(s) there is no flow interruption. It turns out that even in this case a moving jam can be a wide moving one, i.e., the jam propagates through a bottleneck while maintaining the mean velocity of the downstream jam front, if the relation  $\tau_{\text{max}}/\tau_{\text{del}}^{(\text{ac})}$  for the lane(s) with flow interruption within the jam is great enough [19]. Similar results are found for other moving jams in single vehicle data, i.e., for the example measured on the freeway A92-West (Fig. 1 (d)).

In other example shown in Fig. 1 (e), there are also many moving jams during the time intervals of congested traffic. The speed within two moving jams in Fig. 3 is also very low. Nevertheless, rather than wide moving jams these moving jams should be classified as narrow moving jams [1, 19]. This is because there are no traffic flow interruptions within these moving jams (Fig. 3). Indeed, upstream and downstream of the jams, as well as within the jams there are many vehicles that traverse the induction loop detector: There is no qualitative difference in the time-dependences of time headways for different time intervals associated with these narrow jams and in traffic flow upstream or downstream of the jams (Fig. 3 (b, c)). This can be explained if it is assumed that each vehicle, which meets a narrow moving jam, must decelerate at the upstream jam front down to a very low speed within the jam, can nevertheless accelerate at the downstream jam front almost without any time delay within the jam: The narrow moving jam consists of upstream and downstream jam fronts only. These assumptions are confirmed by single vehicle data shown in Fig. 3, in which time intervals between different measurements of time headways and for the value  $3600/\tau^{(\text{gross})}$  for different vehicles exhibit the same behavior away and within the jams [19]. Thus, regardless of these narrow moving jams traffic flow is not discontinuous, i.e., the narrow moving jams belong

indeed to the synchronized flow phase.

A comparison of the microscopic criterion (1) with the macroscopic spatiotemporal criteria for the phases made in [19] allows us to suggest that the moving jam in Fig. 2 for which the criterion (1) is satisfied is associated with the wide moving jam phase: The jam propagates through a bottleneck while maintaining the mean velocity of the downstream jam front. In contrast, narrow moving jams in Fig. 3 for which the criterion (1) is not satisfied are associated with the synchronized flow phase: The narrow moving jam is caught at the bottleneck.

Between flow interruption intervals within the wide moving jam in Fig. 2, vehicles within the jam exhibit time headways about 5 sec or longer. The latter can be explained by moving blanks within the jam. Empirical single vehicle data (Fig. 2) shows that when vehicles meet the wide moving jam, firstly they decelerate at the upstream jam front sharply up to a standstill. As a result, the first flow interruption interval in all lanes appears. It can be assumed that net distances (space gaps) between these vehicles can be very different and the mean space gap can exceed a minimum (safe) space gap considerably. For this reason, later the vehicles become to decrease these space gaps. As a result, low vehicle speed states appear within the jam as this can be seen in Fig. 2 (a, c, e). Consequently, due to this vehicle motion new space gaps, i.e., blanks between vehicles occur upstream within the jam. Then other vehicles that are upstream begin to move within the jam covering these blanks. This lead to occurrence of moving blanks propagating upstream within the jam.

These assumptions are confirmed by low speed states within the jam (Fig. 2 (a, c, e)). These low speed states within wide moving jams associated with moving blanks are not necessarily synchronized between different lanes. For example, in Fig. 2 (a, c, e), in the interval 8:43–8:44 there can be seen non-interrupted traffic flows of low speeds in the middle and right lanes associated with moving blanks within the jam, whereas in the left lane traffic flow is interrupted. Mean time headways related to moving blanks within the jam are usually longer (3–7 sec) than they are away from the jam in free flow and in synchronized flow (Fig. 2 (h)).

### 3. Empirical characteristics of traffic phases

A comparison of average characteristics of low vehicle speeds within a wide moving jam associated with moving blanks (crossing and triangle points) with free flow (black quadrates), synchronized flow (circles), and the line  $J$  for the downstream jam front (line  $J$ ) is presented in Fig. 4, in which a moving averaging of vehicle platoons of five vehicles passing the detector has been performed. As found earlier [20, 21, 22] (see Fig. 1 in [22]), very small density states associated with low vehicle speeds are observed within wide moving jams (crossing points in Fig. 4 (a, b)). Due to these “characteristic” small

density states within wide moving jams (crossing points in Fig. 4 (a, b)) the flow rate is usually in average an increasing function of density in the flow–density plane (crossings plus triangle points in Fig. 4 (a)).

However, a single vehicle analysis of these small density points that has been made allows us to conclude that these points (crossing points in Fig. 4 (a)) as well as the related increasing function of the flow rate with density associated with wide moving jams [22] result from a *large systematic error*. This error is associated with error density estimation within the jams made in [20, 21, 22]. To understand this critical conclusion, recall that due to traffic flow interruption within the wide moving jam some of the time headways are very large (Fig. 2 (b, d, f)). The use of the single vehicle data associated with large time headways for the density estimation through the formula  $\rho = q/v$  ( $q$  and  $v$  are the flow rate and average speed) leads to very small densities with the jam. However, during traffic flow interruption within the jam vehicle do not move; the real density of these standing vehicles is very large. This is because the related measured time headways are not related to time headways between vehicles *moving* in traffic. Thus, the single vehicle data associated with the traffic flow interruption effect within wide moving jams cannot be used for density estimation within the jams. To estimate real vehicle density within a wide moving jam during flow interruption, the density definition (number of vehicles per a freeway length at a given time moment), i.e., *spatial averaging* should be used, rather than density estimation through the use of the formula  $\rho = q/v$  in which the flow rate and average speed are related to *time averaging* of vehicles passing a detector during a given time interval. The spatial averaging (density definition) is not possible to apply, when data is measured at detectors whose locations are far away from each other (Fig. 1 (a)). The conclusion about the large systematic error in density estimation within wide moving jams is confirmed by a numerical analysis made in Sect. II B.

This analysis shows also that within wide moving jams density estimation  $\rho = q/v$  exhibits a relative small error during non-interrupted vehicle motion associated with moving blanks within the jams. This is because in this case the associated time headways are related to vehicles moving within the jams. If only these single vehicle data are used for density estimation, then rather than an increasing function of the flow rate with density (crossing and triangle points in Fig. 4 (a)), the points for moving blanks within the jam associated with random transformations in different directions in the flow–density plane appear (triangle points in Fig. 4 (c, e, g)). This is associated with the physical meaning of low vehicle speed states whose occurrence is due non-regular vehicle motion covering blanks within the wide moving jam.

In Fig. 4, points for synchronized flow are related to synchronized flow states in the jam inflow. The speed in these states is considerably higher than the speed within low speed states associated with moving blanks within

the jam. For this reason, three types of points (for free flow, synchronized flow, and moving blanks within the wide moving jams) appear that are separated one from another in the flow–density and speed–density planes. These separated traffic states for the three traffic phases – free flow, synchronized flow, and wide moving jams – are in accordance with the states on a theoretical double Z-characteristics of three-phase traffic theory (see Sect. 6.4 in [1]), if low speed states within the wide moving jam are taken into account.

However, synchronized flow states can overlap states associated with moving blanks within a wide moving jam (Fig. 5). This is because the speed in synchronized flow states can be as low as the speed in states associated with moving blanks within the jam. Thus, in general case low speed states associated with moving blanks within wide moving jams cannot be used for clear distinguishing the synchronized flow and wide moving jam phases in congested traffic.

## B. Numerical Simulations of Moving Blanks

In numerical simulations presented below, we use the microscopic models and model parameters of Ref. [31, 32]. The main idea of these models is the speed adaptation effect in synchronized flow that takes place when the vehicle cannot pass the preceding vehicle. Within a so-called “synchronization gap”, the vehicle tends to adjust its speed to preceding vehicle without caring, what the precise space gap is, as long as it is safe. Thus, there are an infinity of model steady states at each synchronized flow speed associated with the space gaps between the synchronization and safe gaps, i.e., there is no fundamental diagram for steady state model solutions for synchronized flow in these models. In addition, driver time delay depends on whether a vehicle decelerates or accelerates as well as on the vehicle speed. This enable us to simulate driver behavior in various traffic conditions. A detailed consideration of the models, their physics and parameters can be found in Ref. [31, 32] and Sects. 16.3 and 20.2 of the book [1]. When some other model parameters are used, they are given in figure captions.

For a moving jam in Fig. 6 (a, b), the criterion (1) is satisfied. Indeed, there are two regions in which flow interruption within the jam occur. The maximum time headways (Fig. 6 (c)) associated with these flow interruption effects satisfy the criterion (1) (model time delay  $\tau_{\text{del}}^{(\text{ac})} \approx 1.74$  sec) in the left and right freeway lanes. As a result, in accordance with the macroscopic spatiotemporal criteria for the wide moving jam phase, this jam propagates through an on-ramp bottleneck while maintaining the mean velocity of the downstream jam front.

Within the wide moving jam, between time intervals of flow interruptions there are intervals in which low speed states associated with moving blanks (Fig. 6 (b, c)). As can be seen from vehicle trajectories within the jam, moving blanks are related to a non-regular vehicle motion of

covering blanks between vehicles within the jam (Fig. 7 (a)). These moving blanks propagate upstream with a negative velocity that is in average equal to the characteristic speed of the downstream jam front. During jam propagation, locations of moving blanks as well as their spatial and temporal distributions exhibit complex variations within the jam, which are different in the left and right lanes (Fig. 7 (b, c)); these variations seem to correspond to a random vehicle speed behavior within the jam.

Due to flow interruption within the wide moving jam shown in Fig. 6 (a–c), there is a large error in density distributions calculated through the formula  $\rho = q/v$  in the vicinity of the jam fronts at greater density (curves 2 in Fig. 6 (d)) in comparison with density distributions found based on the density definition (vehicles per freeway length) (curves 1). Indeed, curves 2 in Fig. 6 (d) show a significant density underestimation within moving jams. These error states (crossing points in Fig. 8 (a)) explain the systematic error in the empirical studies of states within wide moving jams made in Ref. [20, 21, 22] that has been illustrated in Fig. 4 (a, b) (compare error points in Figs. 4 (a, b) and 8 (a)).

Only within the regions of moving blanks errors in density distributions calculated through the formula  $\rho = q/v$  (curves 2 in Fig. 6 (d)) in comparison with density distributions found based on the density definition (curves 1) decrease considerably. For this reason, if error states associated with flow interruption within the jam are removed, then remaining states in the flow–density (Fig. 8 (b)) and speed–density planes (Fig. 8 (c)) exhibit a qualitative correspondence with the states within the jam calculated through the density definition (Fig. 8 (d, e)) and related to the speed and density distributions found at a fixed time moment 31.5 min (Fig. 6 (e, f)). Nevertheless, remaining errors lead to some quantitative differences in traffic state determinations within the jam based on detector measurements (Fig. 8 (b, c)) and on the density calculation through the density definition (Fig. 8 (d, e)). In particular, there are points in the flow–density plane found in the density calculation through the density definition (Fig. 8 (d)), which are related to greater density up to the maximum jam density. These points cannot usually be found based on traffic measurements at a detector location (Fig. 8 (b, c)).

To understand possible scenarios of moving blanks emergence within a wide moving jam, spontaneous jam emergence in synchronized flow of an GP at an on-ramp bottleneck has been simulated (Fig. 9). Due to a heterogeneous traffic consisting of vehicles and long vehicles used in these simulations, a moving jam emerges firstly in the right lane only ( $t = 23$  min in Figs. 9 (b, c) and 10 (a)). Then some vehicles in the right lane change to the left lane (arrow 1 in Fig. 10 (a)). On the one hand, this lane changing decreases speed in the left lane. On the other hand, space gaps (blanks) between vehicles in the right lane increase due to lane changing. Vehicles in the right lane begin to cover these blanks ( $t \approx 24$  min

in Fig. 10 (a)). As a result, low speed states within the jam appear associated with these moving blanks. Later, subsequent lane changing of vehicles from the right to the left lane results in an abrupt decrease in speed in the left lane leading to jam formation in this lane (arrow 2 in Fig. 10 (a)). This causes the associated abrupt jam front formation and moving blanks emergence ( $t \approx 25$  min in Figs. 9 (b, c) and 10 (a)). Thus, in this scenario vehicle lane changing from the right to the left lane at the upstream jam front is the main reason for moving blanks emergence within the jam (moving blanks labeled “blanks 1” in Fig. 9 (b)).

During subsequent jam propagation new moving blanks emerge (Fig. 9 (d, e)). Firstly, the upstream jam front in the right lane is upstream of the jam front in the left lane ( $t = 35$  min, Fig. 9 (d, e)). Due to lane changing of vehicles from the right to the left lane, the front locations are synchronized each other (arrow 3 in Fig. 10 (b)). This lane changing causes moving blanks emergence within the jam ( $t = 37$  min, moving blanks labeled “blanks 2” in Fig. 9 (d)).

### III. MOVING JAM FRONTS AND JAM PROPAGATION LOOPS

Whereas within the upstream jam front vehicles decelerate when they met the jam, within the downstream jam front vehicles accelerate escaping from the jam. In simulations made on a single-lane road with an on-ramp bottleneck (Fig. 11), a moving jam is formed in a dissolving general pattern (DGP) that emerges spontaneously at the bottleneck. A platoon of seven vehicles is considered that is going through the moving jam and other traffic states related to the DGP. Within the platoon the density  $\rho$  is calculated at each given time moment, i.e., in accordance with the density definition (vehicles per freeway length). The flow rate associated with the platoon is  $q = \rho v$ , where  $v$  is average vehicle speed within the platoon. It turns out that traffic states in the flow-density and speed-density planes associated with these speed and density within the platoon exhibit two loops labeled *A* and *B* in Fig. 11 (d, e). The loops are associated with different characteristics of the three traffic phases, free flow, synchronized flow, and wide moving jam passing by the vehicle platoon going through the DGP (solid curve in Fig. 11 (a)). These numerical results (Fig. 11 (d, e)) explain empirical results of Treiterer and Myers [16] and Treiterer [17] found in their empirical study of vehicle trajectories within a moving jam, which emerged and propagated upstream of an on-ramp bottleneck [34].

To understand these statements, note that upstream of the bottleneck firstly synchronized flow occurs. Then a narrow moving jam emerges spontaneously in this synchronized flow. During jam propagation, the jam amplitude grows and the narrow moving jam transforms into a wide moving jam, i.e., an S→J transition occurs in the synchronized flow. This wide moving jam prevents

subsequent moving jam emergence in synchronized flow upstream of the bottleneck. As a result, the DGP appears at the bottleneck, which consists of synchronized flow upstream of the moving jam, the moving jam, and synchronized flow that is downstream of the jam and upstream of the bottleneck (Fig. 11 (a)); see a more detailed consideration of the physics of DGP emergence in the book [1]).

Thus, the chosen vehicle platoon (solid curve in Fig. 11 (a)) is going firstly through free flow ( $t < 74$  min in Fig. 11 (a, b)). Secondly, the platoon must decelerate when it reaches synchronized flow, which is upstream of the wide moving jam. In this synchronized flow, speed decreases during the platoon propagation ( $74 < t < 77$  min in Fig. 11 (a, b)). The associated synchronized flow states lie at lower speed and greater density in the flow-density and speed-density planes than the speed and density within the platoon in free flow, respectively (curve 1 in Fig. 11 (d)). Thirdly, the platoon meets the upstream jam front within which the vehicles must decelerate up to the speed within the jam (this speed is almost as low as zero;  $t \approx 78.5$  min in Fig. 11 (a, b)). Consequently, the flow rate and speed sharply decrease and density increases (curve for the upstream jam front in Fig. 11 (d, e)). Later, due to upstream jam propagation through the platoon, the vehicles within the platoon can accelerate at the downstream jam front ( $t \approx 79$  min in Fig. 11 (a, b)). As a result, the flow rate and speed sharply increase and density decreases (curve for the downstream jam front in Fig. 11 (d, e)). We see that at the upstream jam front the flow rate is greater than at the downstream front at the same density. This is because vehicles decelerating at the upstream jam front accept shorter time headways than time headways of vehicles accelerating at the downstream jam front.

Then the platoon moves through synchronized flow downstream of the jam. In this synchronized flow, the speed is lower than in free flow upstream of the jam and downstream of the bottleneck ( $79 < t < 82$  min in Fig. 11 (a, b)). This platoon propagation is also associated with the synchronized flow within the merging region of the on-ramp bottleneck (Fig. 11 (a-c)). Within this region due to the vehicle merging from the on-ramp onto the main road time headways within the platoon decrease. Therefore, the flow rate is a sharply increasing function of freeway location. For this reason, traffic states in the flow-density and speed-density planes associated with the platoon, which is going through synchronized flow downstream of the jam, exhibit rapid flow rate growth with a slightly increasing speed. These synchronized flow states lie at lower speed and greater density in the flow-density and speed-density planes than the speed and density in free flow, respectively (curve 2 in Fig. 11 (d)). This growth of the flow rate results in the loop labeled *A* in the flow-density and speed-density planes. This loop is formed by the upstream and downstream jam fronts together with a part of the curve 2 related to the synchronized flow downstream of the jam (Fig. 11 (d,

e)).

Later, the platoon propagates through the downstream front of synchronized flow in which the speed increases considerably up to the speed in free flow downstream of the bottleneck ( $t \approx 82.5$  min in Fig. 11 (b)). Hence, traffic states in the flow–density and speed–density planes related to the platoon propagating through the downstream front of synchronized flow at the bottleneck exhibit rapid speed growth in the flow–density and speed–density planes (curve 3 in Fig. 11 (d)). Consequently, the platoon propagation through synchronized flow upstream of the jam (curve 1), through synchronized flow downstream of the jam (curve 2), as well as through the downstream front of the synchronized flow at the bottleneck up to free flow downstream of this front (curve 3) lead to the second loop labeled *B* in the flow–density and speed–density planes (Fig. 11 (d)).

Simulations show that loops’ shapes depend on a vehicle platoon that is chosen. If a platoon of seven vehicles is chosen, which propagates earlier through the DGP than the platoon considered in Fig. 11 (b–e), then the loops *A* and *B* (Fig. 12 (a, b)) are different from those in Fig. 11 (d, e). There are several reasons for this result. Firstly, free flow and synchronized flow states upstream and downstream of the jam within the platoon depend on the chosen platoon considerably. Secondly, in Fig. 12 (a, b) the platoon is going through is a narrow moving jam rather than through a wide moving one.

If another platoon of seven vehicles is chosen, which propagates later through the DGP than the platoon considered in Fig. 11 (b–e), then the shape of the loops *A* and *B* (Fig. 12 (c, d)) is different from those in Figs. 11 (d, e) and 12 (a, b). The first reason for this different behavior is the same as those mentioned above. In addition, in this case the platoon is going through a wide moving jam whose width is greater than the width of the wide moving jam associated with the platoon chosen in Fig. 11 (b–e). As a result, there are low speed states within the jam associated with moving blanks within the jam.

In general, due to upstream jam propagation the distance between the downstream jam front and bottleneck location is a time function; in addition, jam characteristics change over time considerably. Thus, average space gaps and speeds within a platoon depend on the time interval, when the platoon is going through a moving jam, through synchronized flows and free flows upstream and downstream of the jam. This can change both loops *A* and *B* in Fig. 12 (a–d) associated with a vehicle platoon going through even the same DGP appreciably. Moreover, the flow rate in free flow downstream of the bottleneck associated with a vehicle platoon can be very different for different platoons. This is due to considerable variations in space gaps between vehicles within different platoons after the platoons have passed the downstream front of synchronized flow at the bottleneck. This explains different flow rates in the free flow associated with three vehicles platoons in Figs. 11 (d) and 12 (a, c). Ap-

parently, this complex loop behavior explains very different loops *A* and *B* observed in the empirical study by Treiterer and Myers [16] and Treiterer [17].

The loops in the flow–density and speed–density planes shown in Fig. 11 (c, d) and 12 (a–d) are associated with measurements of the density within the vehicle platoon in accordance with the density definition (vehicles per freeway length). The use of the density definition is possible, if vehicle trajectories are known as this the case in simulations presented in the article above or in the Treiterer and Myers’s empirical observations of vehicle trajectories [16, 17].

Unfortunately, the use of this correct procedure is not possible to perform, when single vehicle data is measured by a local detector on a road as this the case for the wide moving jam shown in Fig. 2. In this case, the density has to be estimated through the formula  $\rho = q/v$ , in which the flow rate  $q$  and speed  $v$  are associated with time averaging over many *different* vehicle platoons of seven vehicles passing the detector. There are two systematic errors in this case: (i) Density estimation at lower speeds within the jam (see explanations of Fig. 6 (d) in Sect. II B). (ii) Measured and estimated traffic variables associated with different platoons passing the detector do not coincide with the respective traffic variables found for a single vehicle platoon going through the wide moving jam and other traffic phases in Fig. 11.

Apparently these errors lead to qualitative different empirical loops in the flow–density and speed–density planes (Fig. 12 (e)) for the jam shown in Fig. 2 in comparison with empirical observations by Treiterer and Myers [16, 17]. These conclusions are confirmed by numerical simulations in which the same procedure of the density estimation through detector measurements is used (Fig. 12 (f, g)) as those in empirical Fig. 12 (e). The simulated loops in the flow–density and speed–density planes (Fig. 12 (f, g)) associated with traffic variables determined at a detector location within the DGP shown in Fig. 11 (a) are qualitatively different from the loops found through the use of the correct density calculation associated with vehicle platoon propagation through the DGP (Fig. 11 (d, e)).

#### IV. DISCUSSION

Based on empirical and model results presented, the following conclusions can be made:

(i) In empirical observations and numerical simulations, moving blanks that are responsible for low speed states within a wide moving jam exhibit complex a non-regular spatiotemporal behavior. The blanks are often not synchronized between different freeway lanes.

(ii) Lane changing at the upstream front of a wide moving jam can lead to large moving blanks within the jam.

(iii) Moving blanks emergence is characterized by random changes of the upstream jam front location in some of freeway lanes over time.

(iv) To find correct characteristics associated with moving blanks within wide moving jams, measurement points related to the flow interruption effect within the jams leading to a large systematic error in density estimation have to be removed, when wide moving jam characteristics are calculated.

(v) In simulations, there are two loops in the flow–density plane associated with a vehicle platoon propagation through a moving jam as well as through free

flow and synchronized flow states of traffic upstream and downstream of the jam. The loops are associated with different characteristics of the three traffic phases, free flow, synchronized flow, and wide moving jam passing by the platoon. These simulation results made in the context of three-phase traffic theory explain empirical observations of traffic dynamics in vehicle trajectories found by Treiterer and Myers [16] and Treiterer [17].

- 
- [1] B.S. Kerner. *The Physics of Traffic* (Springer, Berlin, New York 2004).
- [2] N.H. Gartner, C.J. Messer, A. Rathi (eds.). *Special Report 165: Revised Monograph on Traffic Flow Theory* (Transportation Research Board, Washington, D.C. 1997).
- [3] D.E. Wolf. *Physica A* **263**, 438 (1999).
- [4] D. Chowdhury, L. Santen, A. Schadschneider. *Physics Reports* **329**, 199 (2000).
- [5] D. Helbing. *Rev. Mod. Phys.* **73**, 1067–1141 (2001).
- [6] T. Nagatani. *Rep. Prog. Phys.* **65**, 1331–1386 (2002).
- [7] K. Nagel, P. Wagner, R. Woesler. *Operation Res.* **51**, 681–716 (2003).
- [8] R. Mahnke, J. Kaupužs, I. Lubashevsky, *Phys. Rep.* **408**, 1–130 (2005).
- [9] H.S. Mahmassani (editor). *Transportation and Traffic Theory*, Proceedings of the 16th Inter. Sym. on Transportation and Traffic Theory (Elsevier, Amsterdam 2005)
- [10] D. Helbing, H.J. Herrmann, M. Schreckenberg, D.E. Wolf (editors). *Traffic and Granular Flow' 99* (Springer, Heidelberg 2000)
- [11] M. Fukui, Y. Sugiyama, M. Schreckenberg, D.E. Wolf (editors). *Traffic and Granular Flow' 01* (Springer, Heidelberg 2003)
- [12] S.P. Hoogendoorn, S. Luding, P.H.L. Bovy, M. Schreckenberg, D.E. Wolf (editors). *Traffic and Granular Flow' 03* (Springer, Heidelberg 2005).
- [13] L.C. Edie, and R.S. Foote. *Highway Res. Board, Proc. Ann. Meeting* **37**, 334 (1958).
- [14] L.C. Edie, R.S. Foote. 'Effect of Shock Waves on Tunnel Traffic Flow'. In: *Highway Research Board Proceedings* **39** (HRB, National Research Council, Washington, D.C. 1960) pp. 492–505.
- [15] L.C. Edie. *Operations Research* **9**, 66–77 (1961).
- [16] J. Treiterer, J.A. Myers. 'The Hysteresis Phenomenon in Traffic Flow'. In: *Procs. 6th International Symposium on Transportation and Traffic Theory*. ed. by D.J. Buckley (A.H. & A.W. Reed, London 1974) pp. 13–38.
- [17] J. Treiterer. 'Investigation of Traffic Dynamics by Aerial Photogrammetry Techniques'. Ohio State University Technical Report PB 246 094, Columbus, Ohio (1975).
- [18] M. Koshi, M. Iwasaki, I. Ohkura. 'Some Findings and an Overview on Vehicular Flow Characteristics'. In: *Procs. 8th International Symposium on Transportation and Traffic Theory* ed. V. F. Hurdle, et al (University of Toronto Press, Toronto, Ontario 1983) pp. 403.
- [19] B. S. Kerner, S. L. Klenov, A. Hiller, e-print: physics/0507094 (2005); *J. Phys. A* (submitted) .
- [20] L. Neubert, L. Santen, A. Schadschneider, M. Schreckenberg. *Phys. Rev. E* **60**, 6480 (1999).
- [21] W. Knospe, L. Santen, A. Schadschneider, M. Schreckenberg. *Phys. Rev. E* **65**, 056133 (2002).
- [22] W. Knospe, L. Santen, A. Schadschneider, M. Schreckenberg. *Phys. Rev. E* **70**, 016115 (2004).
- [23] R. J. Cowan. *Trans. Rec.* **9**, 371–375 (1976).
- [24] T. Luttinen. *Transportation Res. Rec.* **1365** (1992).
- [25] P.H.L. Bovy (editor). *Motorway Analysis: New Methodologies and Recent Empirical Findings* (Delft University Press, Delft 1998).
- [26] B. Tilch, D. Helbing, in: [10], p.333.
- [27] J. Banks. *Trans. Rec. B* **37**, 539–554 (2004).
- [28] G.S. Gurusinghe, T. Nakatsuji, Y. Azuta, P. Ranjitkar, Y. Tanaboriboon. 'Multiple Car-Following Data Using Real-Time Kinematic Global Positioning System'. In: *Preprints of the 82nd TRB Annual Meeting* TRB Paper No.: 03-4137 (TRB, Washington D.C. 2003).
- [29] Sometimes for better statistical conclusions, traffic variables obtained from various days or/and many different locations are aggregated to a data set; this data base of aggregated data is further used for calculation of traffic flow characteristics.
- [30] B. S. Kerner. *Phys. Rev. E* **65**, 046138 (2002).
- [31] B.S. Kerner, S.L. Klenov, *Phys. Rev.* **68** 036130 (2003)
- [32] B.S. Kerner, S.L. Klenov, *J. Phys. A: Math. Gen.* **37** 8753–8788 (2004).
- [33] From a comparison of a local traffic dynamics measured at D7 with the dynamics at D10 in Fig. 1 (b) it has been found that the moving jams propagate upstream with the mean velocity of the downstream jam fronts  $v_g \approx -15.8$  km/h.
- [34] It must be noted that in accordance with traffic flow theory development in the 70'ies, Treiterer and Myers [16, 17] associated loops in the flow–density and speed–density relationships, which they found in observations of vehicle platoon going through a moving jam, with “hysteresis phenomena” in traffic flow. However, from three-phase traffic theory we know now that hysteresis phenomena in traffic flow are associated with the  $F \rightarrow S$  and  $S \rightarrow J$  transitions as well as with different reverse transitions like  $F \rightarrow J \rightarrow F$ ,  $S \rightarrow J \rightarrow S$ ,  $S \rightarrow J \rightarrow F$ , or  $F \rightarrow J \rightarrow S$  transitions [1]. As can be seen from simulations presented in Fig. 11, the loops in the flow–density plane are caused by vehicle platoon propagation through different traffic flow phases (free flow, synchronized flow, and wide moving jam), which can already be formed in traffic, rather than by one of the types of the phase transitions.

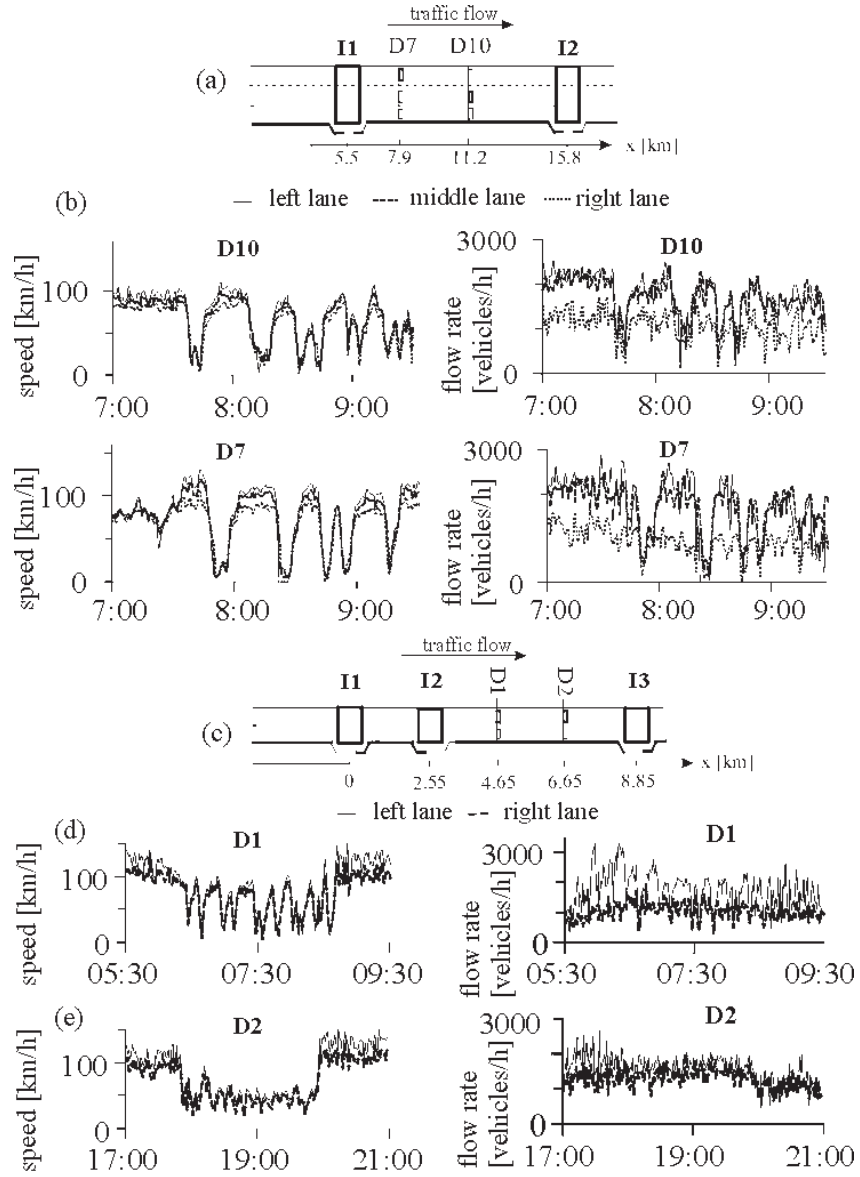


FIG. 1: Macroscopic characteristics of empirical single vehicle data measured on the freeway A5-South (a, b) and on the freeway A92-West (c-e): (a) – Sketch of detector arrangement of a section on the freeway A5-South. (b) – Local traffic dynamics (one-minute average data) of the speed (left) and flow rate (right) in three freeway lanes on December 12, 1995. (c) – Sketch of detector arrangement on a section of the freeway A92-West. (d, e) – Local traffic dynamics (one-minute average data) of the speed (left) and flow rate (right) on July 17, 2000 (d) and August 23, 2000 (e) in both freeway lanes.



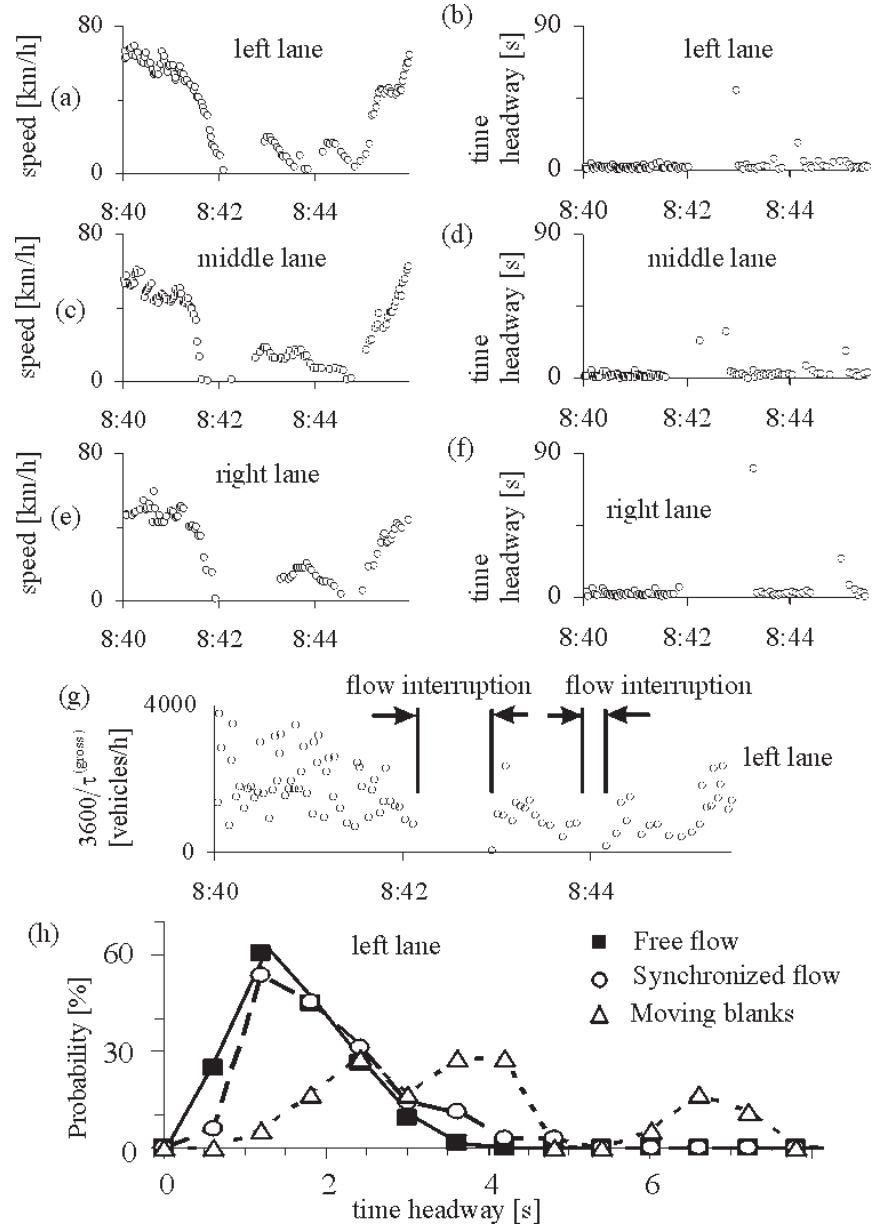


FIG. 2: Microscopic structure of wide moving jams: (a–f) – Empirical single vehicle data for speed within a wide moving jam (a, c, e) and the associated time headways (b, d, f) in the left (a, b), middle (c, d), and right lanes (e, f) related to the example at D10 in Fig. 1 (b). (g) – Time distributions of the value  $3600/\tau^{(\text{gross})}$  in the left lane. (h) – Probability for time headways in the left lane for free flow (solid curve,  $6:20 \leq t \leq 6:40$ ), synchronized flow (dashed curve,  $8:39 \leq t \leq 8:42$ ); moving blanks within the wide moving jam (dotted curve,  $8:42 < t \leq 8:44$ ).

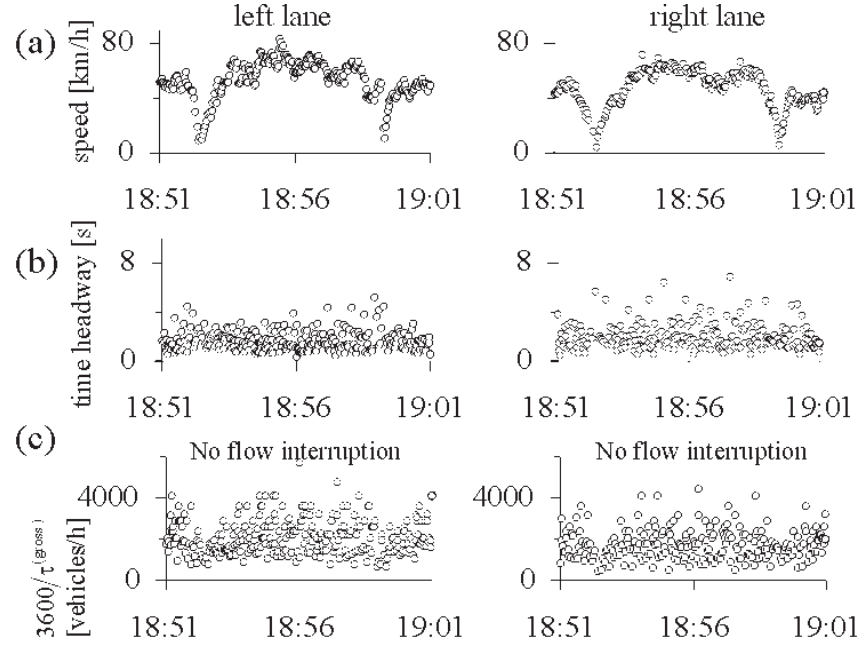


FIG. 3: Microscopic structure of narrow moving jams: Empirical single vehicle data for speed within a sequence of two narrow moving jams in the left (left) and right lanes (right) (a) as well as the associated time distributions of time headways  $\tau$  (b) and of the value  $3600/\tau^{(\text{gross})}$  (c) related to Fig. 1 (e).

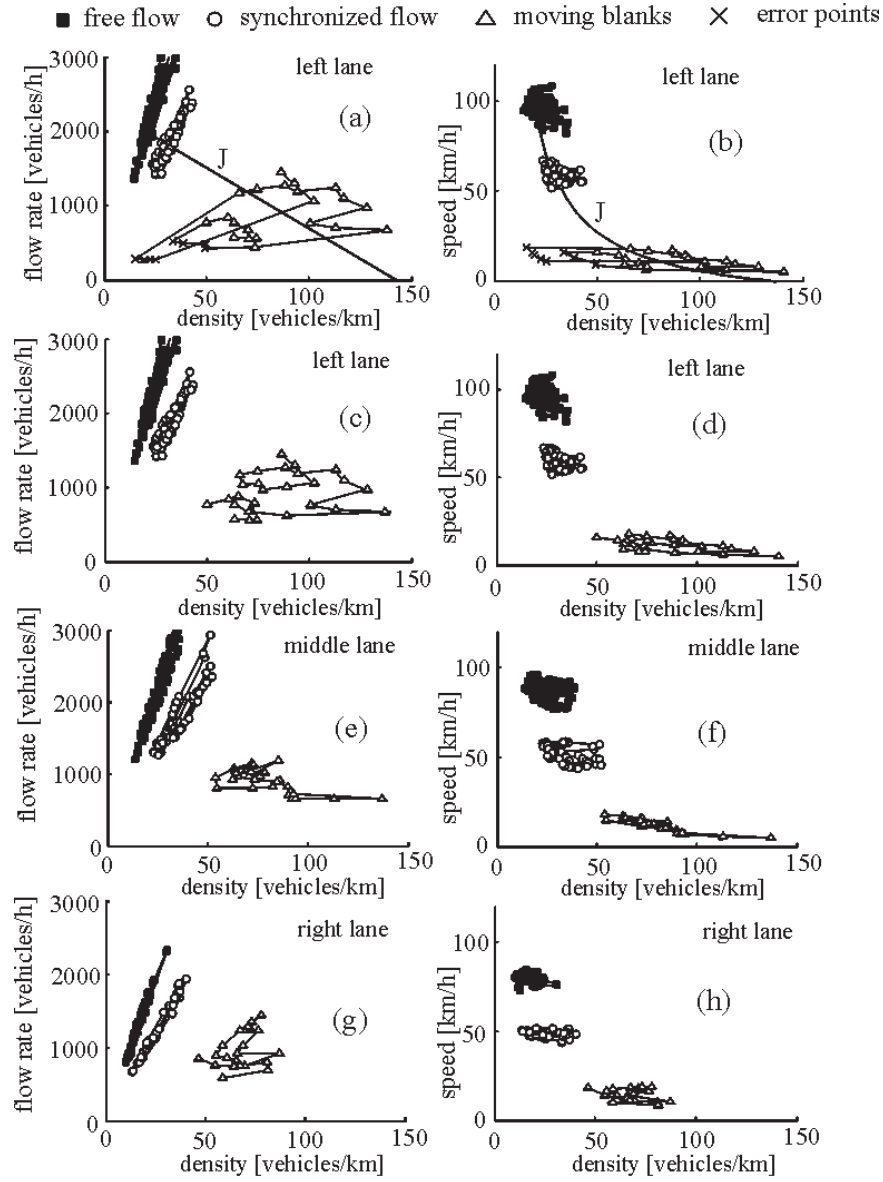


FIG. 4: Empirical characteristics of traffic phases: (a, b) – Traffic phases in the flow–density (a) and speed–density (b) planes for data in the left lane together with the line  $J$  (a) and the curve  $J$  (b) associated with the propagation of the downstream front of the wide moving jam. (c–g) – Traffic phases in the flow–density (c, e, g) and speed–density (d, f, h) planes for *improved data* in the left (c, d), middle (e, f), and right (g, h) lanes. Moving averaging over the platoon of five vehicles is used.

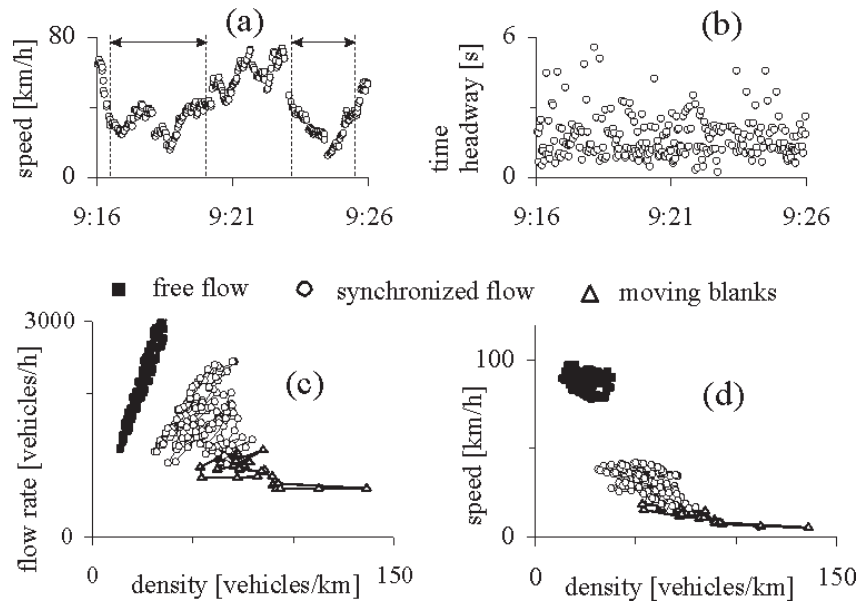


FIG. 5: Empirical characteristics of traffic phases: (a, b) – Single vehicle data for speed (a) and time headways (b) for synchronized flow at D10 related to Fig. 1 (b). (c, d) – Traffic states averaged over five vehicles (moving average) associated with synchronized flow in (a) and with moving blanks within the jam taken from Fig. 4 (e, f) in the flow–density (c) and speed–density planes (d). Arrows in (a) show time intervals of synchronized flow states used in (c, d). Middle freeway lane.

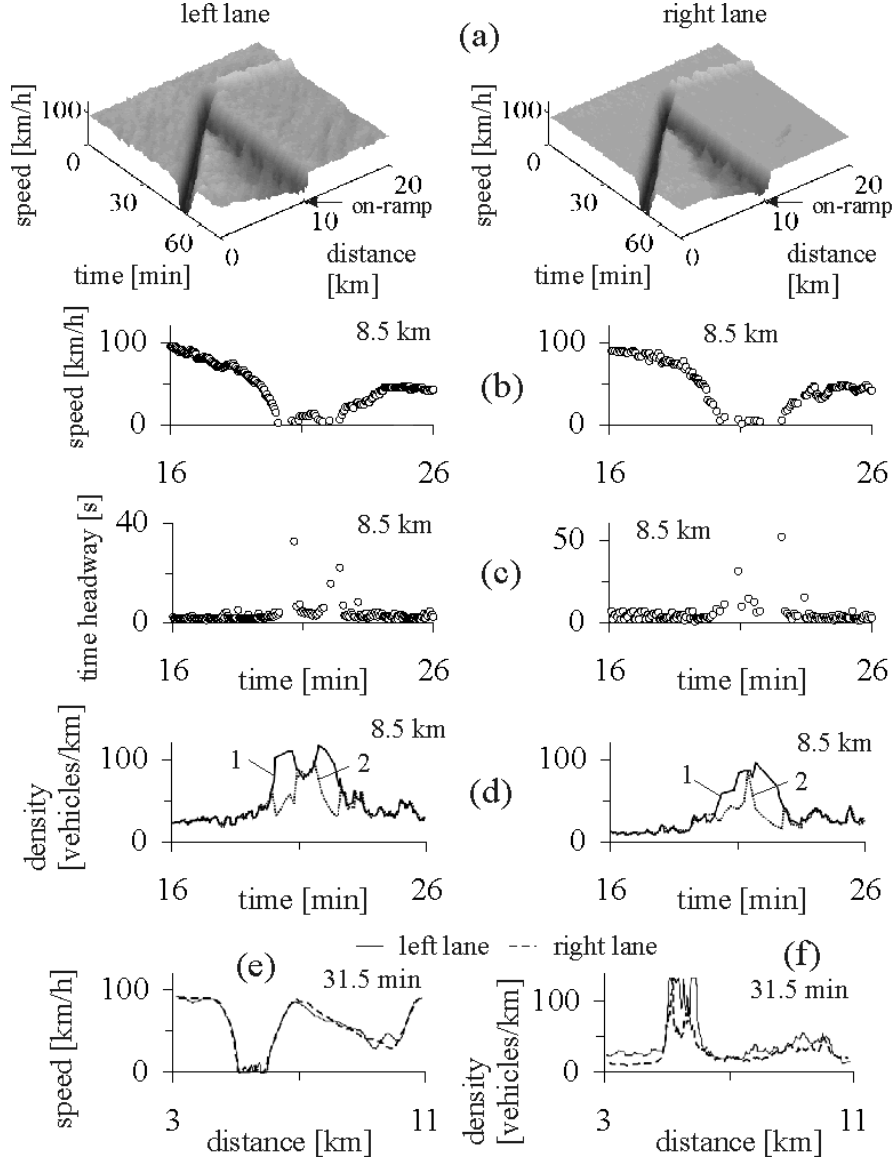


FIG. 6: Simulations of moving blanks within a wide moving jam propagating through an on-ramp bottleneck. (a) – Speed in space and time on the main road. (b–d) – Single vehicle data for time dependencies of speed (b), time headways (c), and the associated density distributions calculated through the density definition (curves 1) and the formula  $\rho = q/v$  (curves 2) (d) at the location 8.5 km. Left and right figures (a–d) are related to the left and right lanes, respectively. In (d) for density calculation, a moving averaging over the platoon of five vehicles is performed. To use the density definition by calculations of curves 1 in (d), at a time moment when one of the vehicles has just been detected at the location 8.5 km the density within a vehicle platoon is calculated. This platoon consists of the detected vehicle and two vehicles upstream and two vehicles downstream. In contrast, calculations of curves 2 in (d) are performed as in empirical observations in Fig. 4, i.e., the flow rate  $q$  and average speed  $v$  of the platoon passing the location are used in the formula  $\rho = q/v$ . (e, f) – Speed (e) and density (f) related to (a) as functions of distance at the time moment 31.5 min in the left and right lanes. Model for heterogeneous traffic of Sect. 20.2 in [1] with 80% fast and 20% long vehicles;  $\tau_{\text{del}}^{(a,j)}(v) = \tau/p_0^{(j)}(v)$ ,  $p_0^{(j)}(v) = (a^{(j)} + b^{(j)} \min(1, v/10))$ ,  $j = 1, 3$ ;  $a^{(1)} = 0.565$ ,  $b^{(1)} = 0.085$  for fast vehicles ( $j = 1$ ), and  $a^{(3)} = 0.3$ ,  $b^{(3)} = 0.18$  for long vehicles ( $j = 3$ ).  $q_{\text{in}} = 1565$ ,  $q_{\text{on}} = 337$  vehicles/h/lane.  $q_{\text{out}} = 1900$  and  $q_{\text{out}} = 1100$  vehicles/h in the left and right lanes, respectively. On-ramp location is  $x_{\text{on}} = 10$  km, on-ramp merging region length is  $L_m = 300$  m. The wide moving jam is exited by local perturbations applied in both lanes; perturbation duration  $T^{(\text{pert})}$  and their location  $\Delta x^{(\text{pert})}$  downstream of the end of the on-ramp merging region are: (3 min, 1250 m).

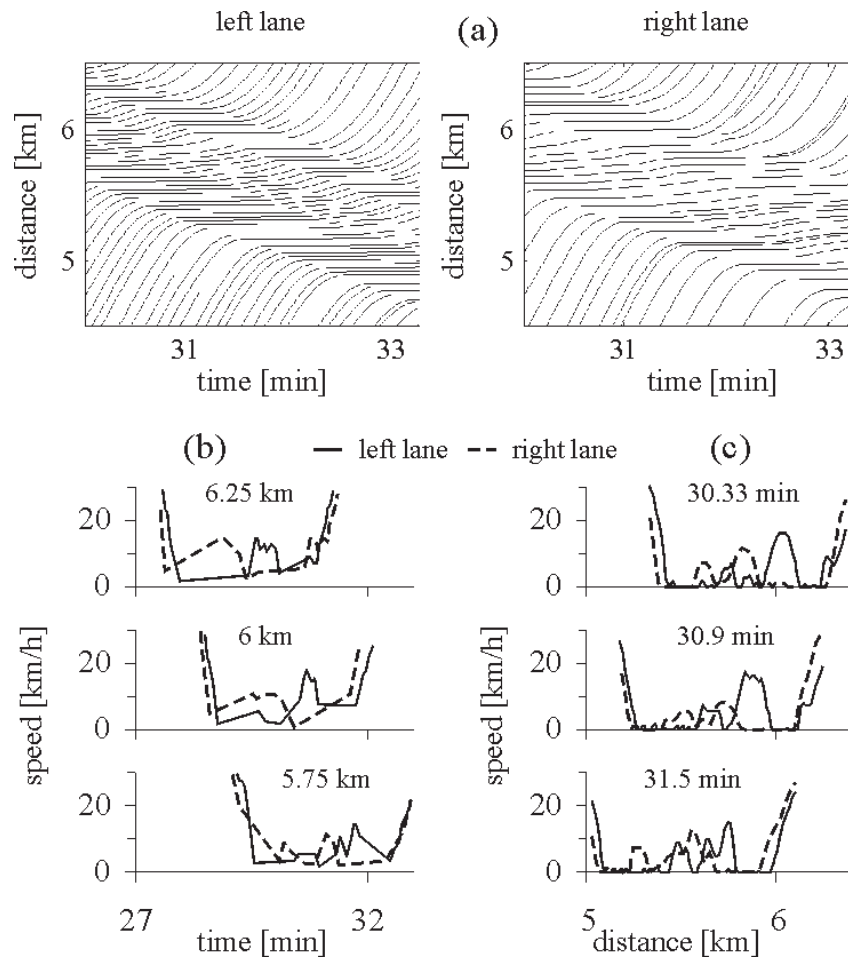


FIG. 7: Microscopic characteristics of moving blanks within the wide moving jam shown in Fig. 6 (a): (a) – Vehicle trajectories in the left (left) and right (right) lanes. (b, c) – Moving blanks at three different locations (b) and three different time moments (c) in the left and right lanes. Trajectories of each 4th vehicle are shown.

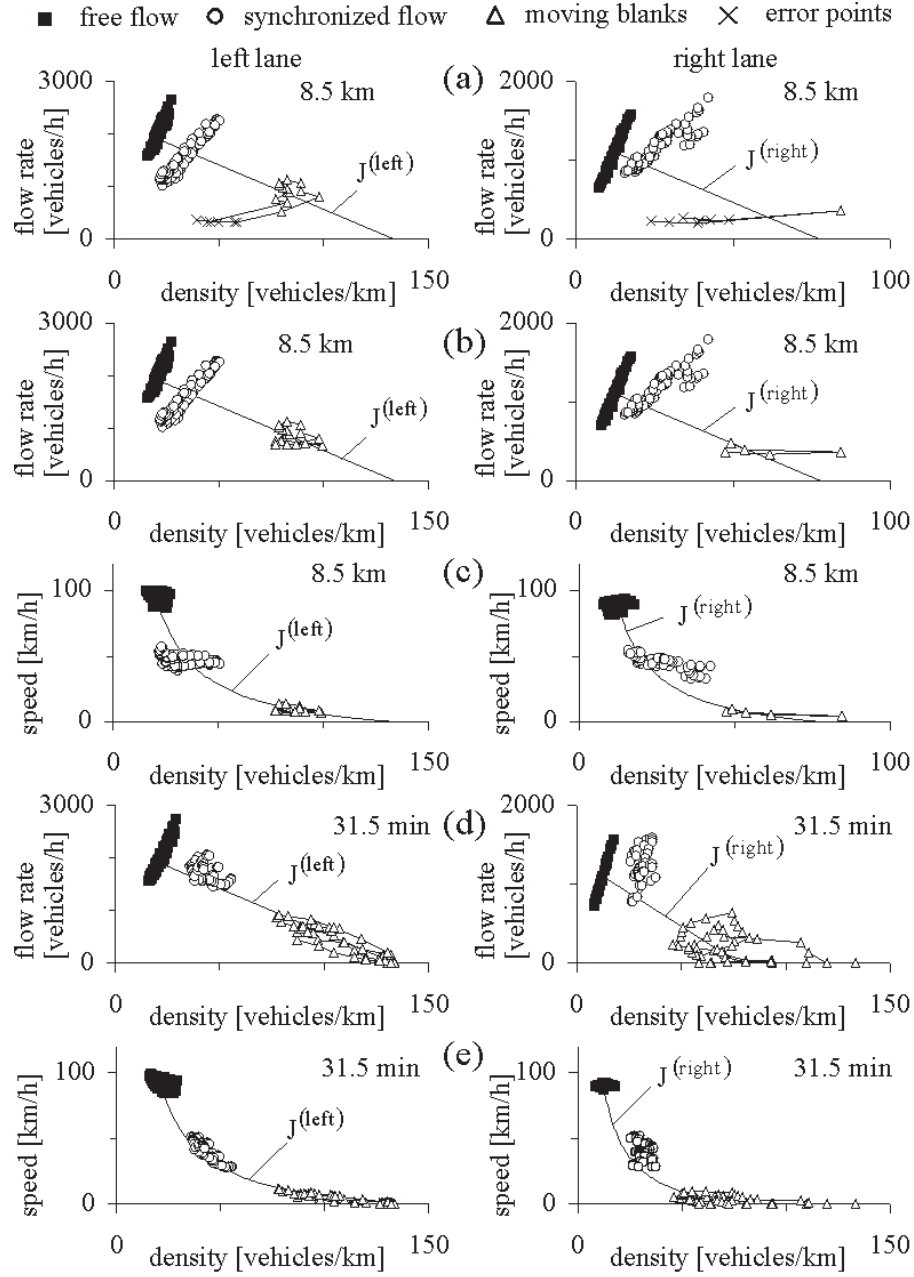


FIG. 8: Characteristics of moving blanks within the wide moving jam shown in Fig. 6 (a) together with states of free flow and synchronized flow in the flow–density (a, b, d) and speed–density planes (c, e). Left and right figures are related to the left and right lanes, respectively: (a–c) – States within the jam are determined at detector located at 8.5 km through the formula  $\rho = q/v$  in two cases in which all states within the jam measured at the detector are shown (a) and error states are removed (b, c). (d, e) – States within the jam are determined through the density definition (vehicles per freeway length) at time moment 31.5 min. Moving average over five vehicles in vehicle platoons is used.  $J^{(\text{left})}$  and  $J^{(\text{right})}$  are the line  $J$  (a, b, d) and the associated curve  $J$  (c, e) for the downstream jam front in the left and right lanes, respectively.

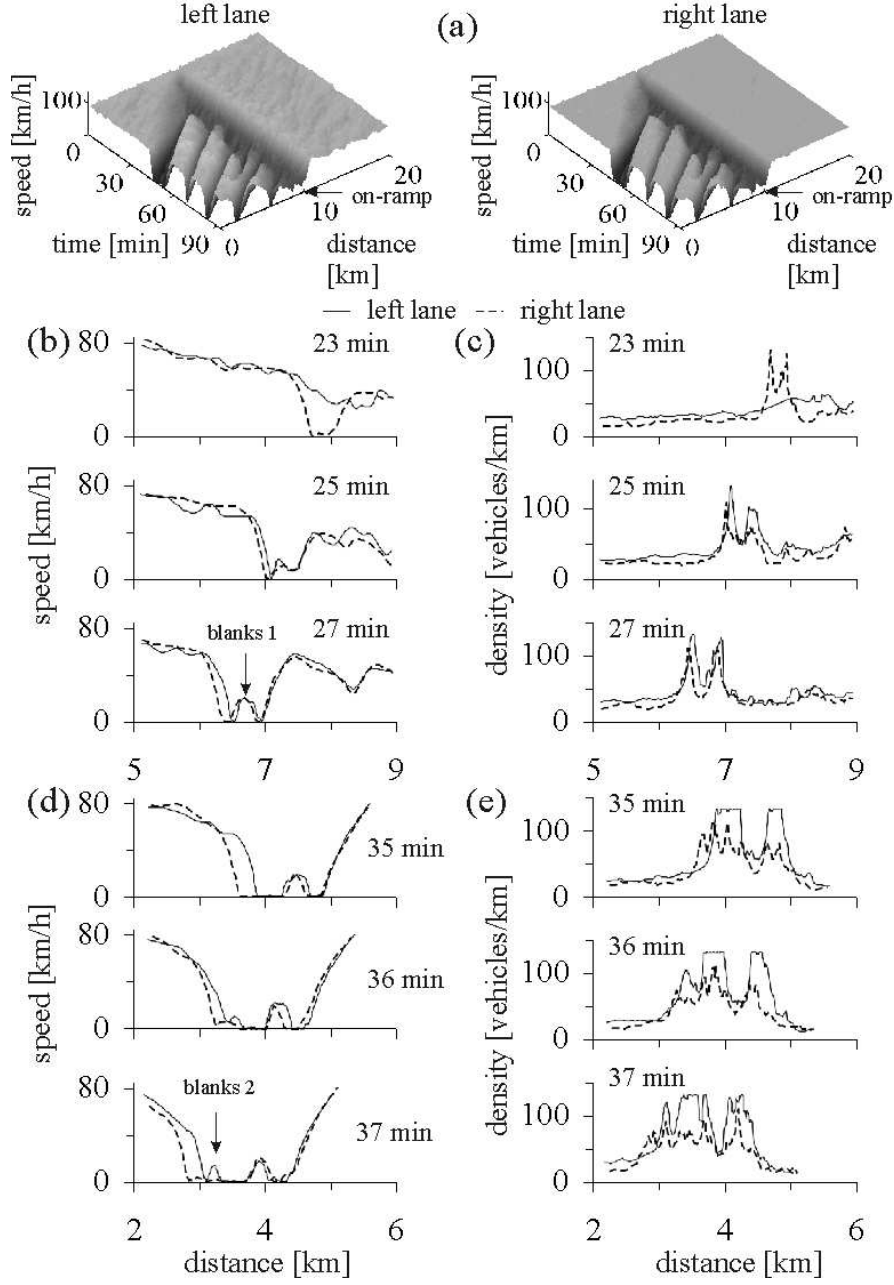


FIG. 9: Simulations of moving blanks emergence: (a) – Speed in space and time within general pattern (GP) at on-ramp bottleneck in the left (left) and right lanes (right). (b–e) – Speed (b, d) and density (c, e) determined through the use of the density definition (vehicles per freeway length) at different time moments associated with the GP in (a) in the left and right lanes.  $q_{in} = 1714$ ,  $q_{on} = 450$  vehicles/h/lane. Model and bottleneck parameters are the same as those in Fig. 6.



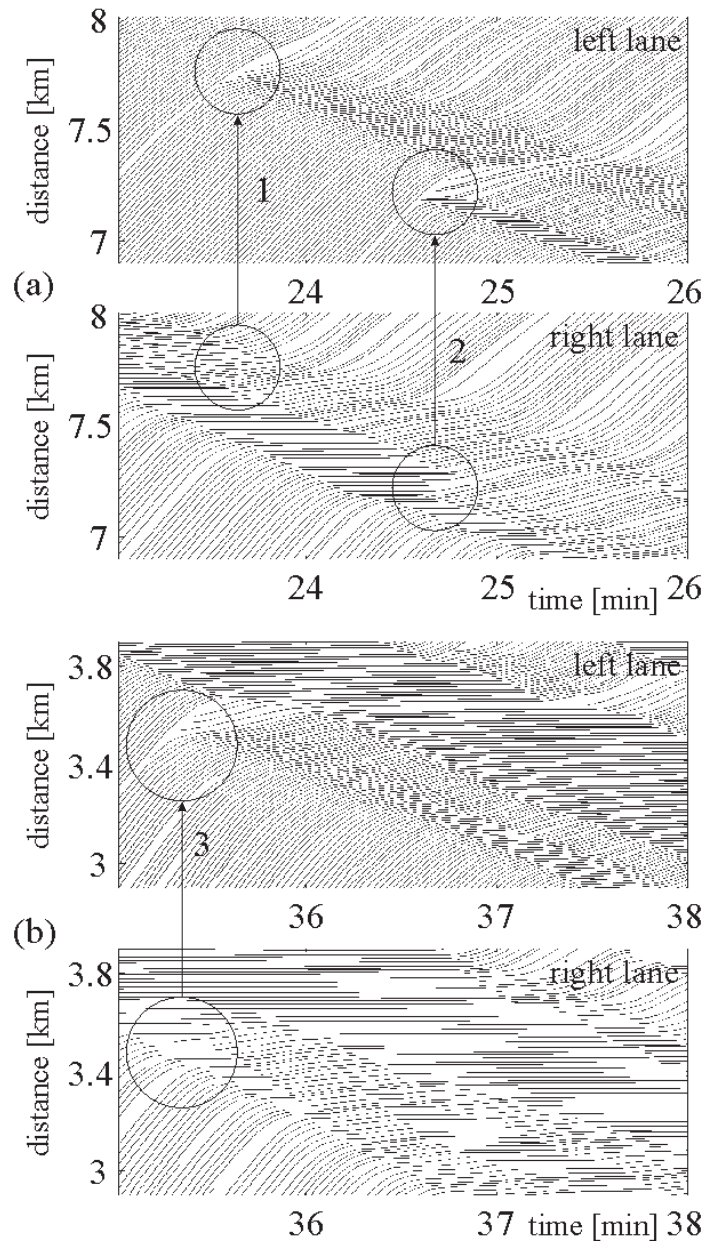


FIG. 10: Moving blanks emergence in the GP shown in Fig. 9 (a): (a, b) – Vehicle trajectories for different time intervals in the left and right lanes.

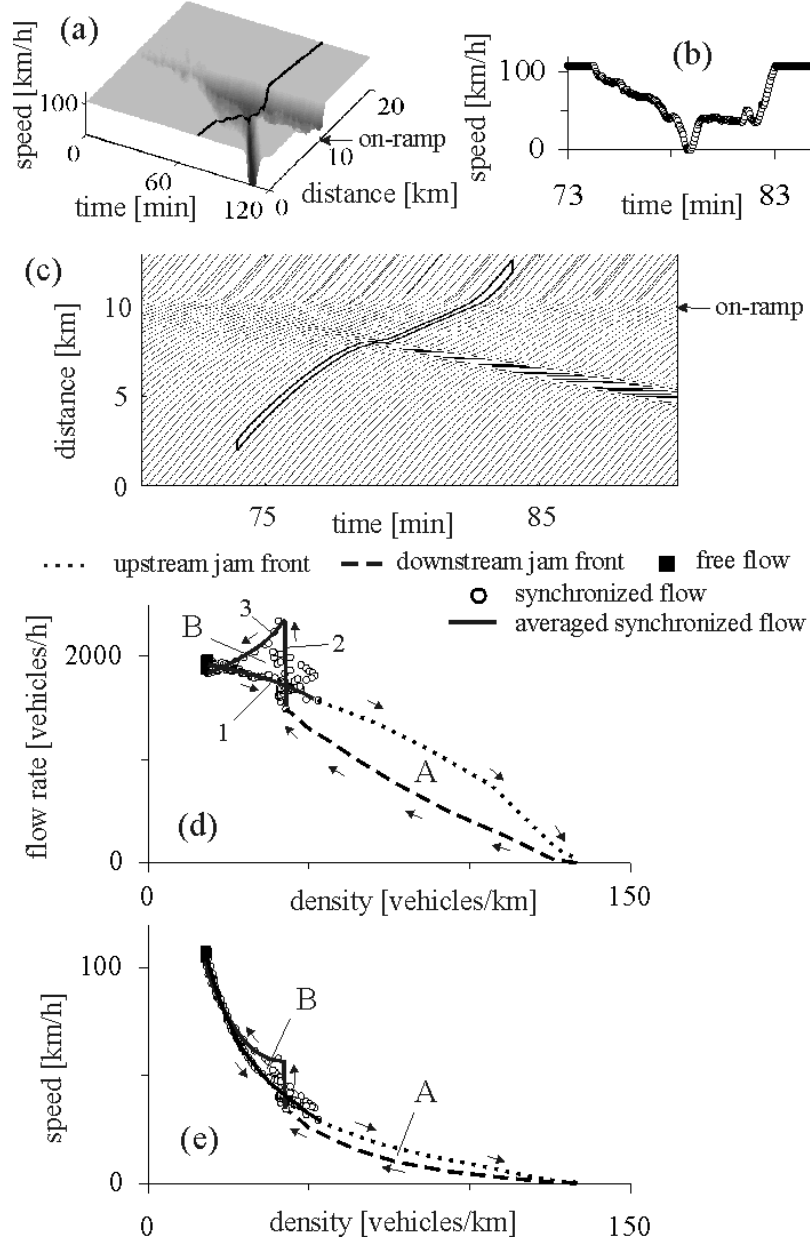


FIG. 11: Microscopic features of moving jam propagation: (a) – Speed on the main road in time and space related to a dissolving general pattern (DGP) that emerges spontaneously at an on-ramp bottleneck. (b) – Speed within a platoon of seven vehicles propagating through the wide moving jam and synchronized flow phases formed in the DGP; speed is averaged over the vehicle platoon. Solid curve in (a) shows the average trajectory associated with platoon propagation. (c) – Vehicle trajectories within the DGP in which the vehicle platoon related to (b) is marked by solid block. (d, e) – Flow–density (d) and speed–density relationships (e) associated with the platoon of seven vehicles going through the wide moving jam and synchronized flow phases related to the DGP in (a–c). Single-lane model of identical vehicles (Sect. 16.3 of Ref. [1]).  $q_{in} = 1946$ ,  $q_{on} = 345$  vehicles/h.  $x_{on} = 10$  km,  $L_m = 300$  m. In (c) trajectories of each 10th vehicle are shown.

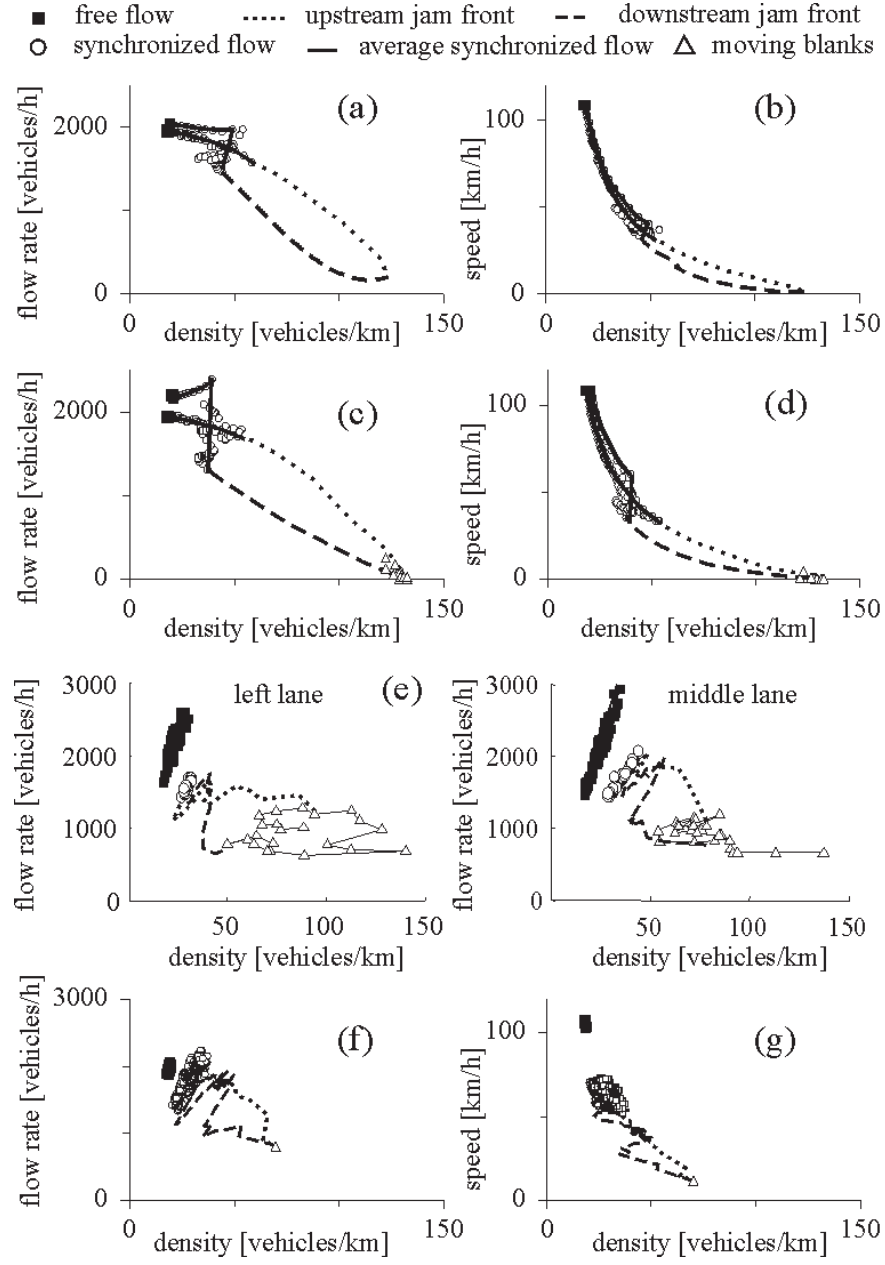


FIG. 12: Simulated flow–density (a, c) and speed–density relationships (b, d) of two different platoons of seven vehicles going through the wide moving jam and other traffic phases within the DGP shown in Fig. 11 (a). (e) – Empirical flow–density relationships in the left and middle lanes associated with the wide moving jam in Fig. 2. (f, g) – Simulated flow–density (f) and speed–density relationships (g) associated with moving averaging of speed  $v$  and flow rate  $q$  within platoons of seven vehicles going through a virtual detector at  $x = 8$  km within the DGP shown in Fig. 11 (a).